Multispectral Imaging with Flash Light Sources

Johannes Brauers[a], Stephan Helling[b] and Til Aach[a]

[a] Institute of Imaging & Computer Vision, RWTH Aachen University, Templergraben 55, D-52056 Aachen, Germany
[b] Color and Image Processing Research Group, RWTH Aachen University, Templergraben 55, D-52056 Aachen, Germany

Abstract

Flash photography is widely used in professional studios due to its high intensities and the resulting short exposure times. However, most multispectral image acquisition systems use continuous light sources. But since flashguns exhibit several advantages over heat light sources, namely high intensities at short firing times, low heat production and small aperture stops, we developed a multispectral flash acquisition system: We use a multispectral camera with a bandpass filter wheel and sequentially acquire grayscale images, which are then combined into a multispectral image. For each filter wheel position, we trigger the flash. The colorimetric analysis of the estimated spectra shows that flash light multispectral imaging performs comparably to a heat light source system, with a mean color error of $\Delta\bar{E}_{00} = 1.594$. *We consider several aspects specific to flash light sources, namely the spectrum, repeat accuracy, illumination uniformity, calibration of the system, interference stripes and synchronization.*

Introduction

Typical light sources for multispectral imaging systems are halogen, HQI (hydrargyrum quartz iodide) [1] and HMI (hydrargyrum medium-arc iodide) lamps [2]. Since the amount of light reaching the imaging sensor is drastically reduced by the optical bandpass filters used to sample the spectrum, only lamps with high power output provide a sufficient amount of light at the sensor thus generating considerable heat. This complicates the usage of bandpass filters in front of the light source instead of the optical path of the camera. The latter alternative causes optical aberrations [3] and focusing problems. On the other hand, a reduced lamp power output requires large exposure times, slows down acquisition and makes the acquisition of moving objects impossible due to motion blur.

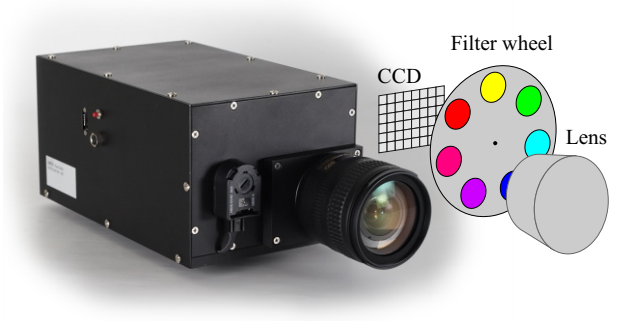

Figure 1. *Our multispectral camera with its internal configuration sketched.*

We therefore discuss a multispectral acquisition system using a flash light source. Since a typical flashgun emits the quantity of light required for an exposure in a very short interval, the overall acquisition time can be drastically reduced. In addition, short exposure times reduce the risk of blurring the image, which might be caused by vibrations. Optical filters can be positioned in front of the small aperture of a flashgun and are not affected by heat. However, multispectral flash acquisition requires a controlled environment.

Image Acquisition

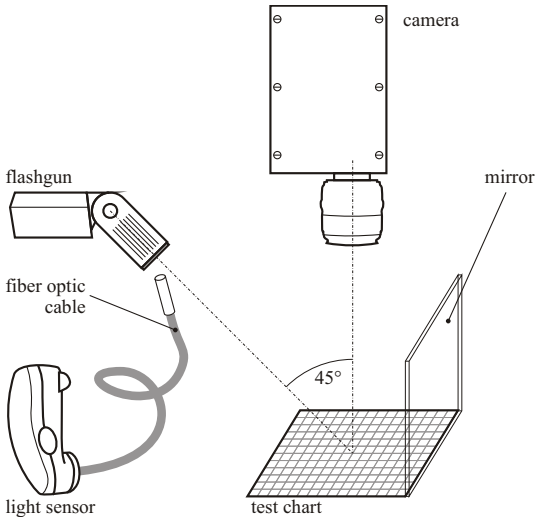

Figure 2. *Acquisition setup.*

For flash image acquisition we use the setup depicted in Fig. 2, which basically represents a 45°/0° setup. Our multispectral camera is mounted perpendicular to the object plane, whereas the flashgun is placed at a 45° angle with respect to the optical axis of the camera to reduce specular reflections on the test object. To improve the uniformity of the illumination, we placed a mirror on the opposite side of the flashgun. To additionally measure the intensity, we positioned a fiber optic cable in front of the flashgun, which is connected to a light sensor. Our multispectral camera internally uses a filter wheel with seven optical bandpass filters and is sketched in Fig. 1.

The acquisition of a multispectral image with the described system works as follows: For each optical passband, the appropriate optical filter is selected via software. After positioning, both camera and spectral photometer are triggered. The exposure end point of both devices should exceed the flash duration and depends on the firing time as well as the delay between camera exposure start and flash trigger. Finally, the flash is fired with the appropriate intensity, which has to be estimated in advance. These steps are repeated for each one of the seven optical filters, resulting in seven grayscale images, we call spectral *frames*, where each *frame* represents the image information for one spectral passband.

To compensate for various camera- and illumination-

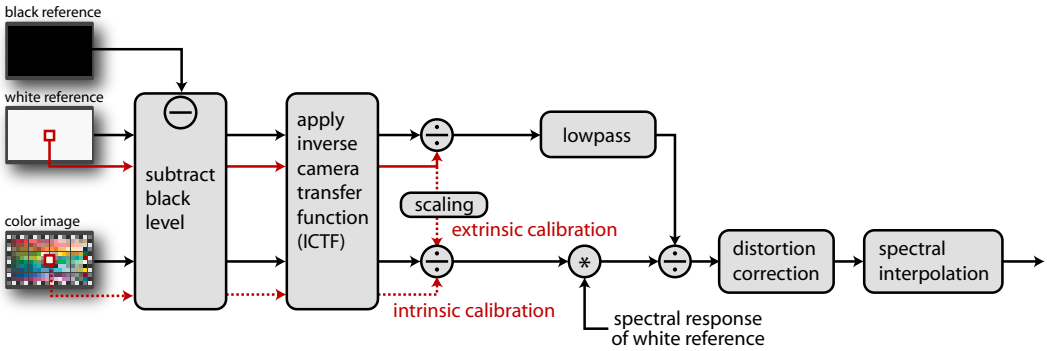

Figure 3. *Processing pipeline.*

specific irregularities, we acquire a black and white reference image. The black reference image is taken with the lens cap attached to the lens and enables us to compensate for the black point of the camera. For the acquisition of the white reference, we acquire a homogeneous white plate and determine the shading of the image to compensate for illumination inhomogeneities. Additionally, the white plate serves as a spectral reference to calibrate our system to the illumination.

Our experiments (see below) show that the flash intensity varies for consecutive exposures, necessitating a calibration procedure. A light sensor with a linear characteristic curve (or – in our case – a spectral photometer) serves as a reference, measuring the flash intensity parallel to the camera. While the camera pixel intensities normally depend on the object being imaged, the light reference sensor only measures the intensity of the light source. We correct each image by a factor determined from the intensity measured by the light sensor.

The processing pipeline for the reconstruction of a multispectral image taken with our flash camera is shown in Fig. 3. Background information and a mathematical description of the postprocessing may be found in [4] and [5]. The black and white reference image and the color image are the input data of our processing. The black reference image is a single grayscale image, whereas the other ones are seven grayscale *frames* representing the seven spectral passbands. To compensate for the (spatially varying) black point, the black reference is subtracted from both the white reference and the color image. After that, we apply the inverse *camera transfer function* (CTF) to both images to compensate for non-linearities of the camera: The CTF – also known as opto-electronic conversion function (OECF) – describes the relation between irradiance values impinging on the camera sensor and the digital output values transferred to the computer. Our measurement stand described in [4] enables us to measure the typical non-linearities of a camera.

Since the intensity of the flash varies – both intentionally and because of accuracy problems – and the optical filters exhibit different transmission curves, we adapt the brightness of the white reference image with an averaged value from the center of the image. The patch is denoted with a red rectangle in Fig. 3; of course, the data in this patch is also preprocessed with the black level and CTF compensation. By dividing the white reference image by the values taken from this area, all spectral frames, i.e., all grayscale images corresponding to their spectral passbands, now exhibit the same brightness value in the center region and may be used for a shading correction of the color image. The scaling can also be interpreted as a multispectral white balance. To remove small speckles and to reduce noise, we additionally apply a lowpass filter to the white reference image.

For the calibration of the color image (which may also be interpreted as a multispectral white balance), we propose two different techniques – *intrinsic* and *extrinsic* calibration. The first one works similar to the calibration of the white reference image and requires a reference patch in the acquired scene. In our test image, we used the white patch in the center of the ColorChecker DC and divided the color image by the averaged spectral values of this patch. Intrinsic calibration does not require the measurements of the external sensor shown in Fig. 2.

Extrinsic calibration relies on the reference values taken in the center of the white reference card (and not the ColorChecker DC). Because of the temporal variation of the flash intensity, which causes different exposures of the white reference and color frames, we have to take the external measurements from the light sensor into account: Let $\mathbf{H} = (\mathbf{H}_1 \dots \mathbf{H}_I)^T$ be an $(I \times N)$ matrix containing the $I = 7$ spectral sensitivity curves for the bandpass filters including the spectral characteristic of the sensor, where each curve vector $\mathbf{H}_i$ $(N \times 1)$ has N sampling points and $i = 1 \dots I$. Typically we use $N = 61$ sampling points covering a wavelength range from $\lambda_1 = 400$nm to $\lambda_N = 700$nm in steps of 5nm. Since the intensity of the flash may vary each time we fire the flashgun, we have to consider the spectrum of the light source for each trigger and denote it as $\mathbf{S} = (\mathbf{S}_1 \dots \mathbf{S}_I)$, where each $\mathbf{S}_i$ is a vector $(N \times 1)$ with the spectrum of the light source. The vector with the scaling factors denoted in Fig. 3 then is computed by

$$f = \frac{\operatorname{diag}(\mathbf{H}\mathbf{S}_{\text{testchart}})}{\operatorname{diag}(\mathbf{H}\mathbf{S}_{\text{whiteref}})}, \tag{1}$$

where diag is a diagonal operator returning the diagonal elements of a matrix and the fraction bar has to be interpreted as an element-wise division. In other words the camera white reference values taken from the white reference card corresponding to the flash intensities $\mathbf{S}_{\text{whiteref}}$ specific for this particular acquisition are *related* to the ones $\mathbf{S}_{\text{testchart}}$ for the color image. Our experiments in Fig. 4 further show that the spectrum is scaled uniformly for different flash intensities; therefore we can use a simple light sensor instead of a photometer and Eq. (1) reduces to

$$f = \frac{\mathbf{v}_{\text{testchart}}}{\mathbf{v}_{\text{whiteref}}}, \tag{2}$$

where $\mathbf{v}_{\text{testchart}}$ $(I \times 1)$ are the light sensor measurement values for the color image and $\mathbf{v}_{\text{whiteref}}$ are the ones for the white reference image.

The calibration of the color image above resembles a white balance for multispectral images. But since the spectrum of the

white reference card typically does not exhibit a perfect *white* spectrum, e.g., has a higher absorption in the blue color range, it has to be multiplied with the multispectral data [4] as shown in Fig. 3. To compensate for the (slightly) inhomogeneous illumination of the test target, we furthermore divide the color image by the lowpass-filtered white reference image.

Since the optical bandpass filters in our camera (see Fig. 1) exhibit different thicknesses and refraction indices, may be tilted with respect to the optical axis and are located between CCD and lens, we have to compensate for the resulting optical aberrations. Towards this end, we use our physical model developed in [3] to analyze and compensate for the distortions. Finally, we estimate the spectrum for each image pixel with a Wiener inverse [5], which accounts for smooth reflectance spectra.

Practical Considerations

We measured the spectrum of our flashgun Sigma EF-500 DG Super [1] at varying intensities (see Fig. 4) with a Dr. Gröbel[2] spectral photometer, which has a spectral range from 200nm to 800nm with a resolution of 0.6nm. To be able to compare the spectra, we normalized the emission curves and plotted them into one figure – the original curves are shown in the small box. Except for the peaks, the spectrum is very similar; we did not notice a color temperature shift.

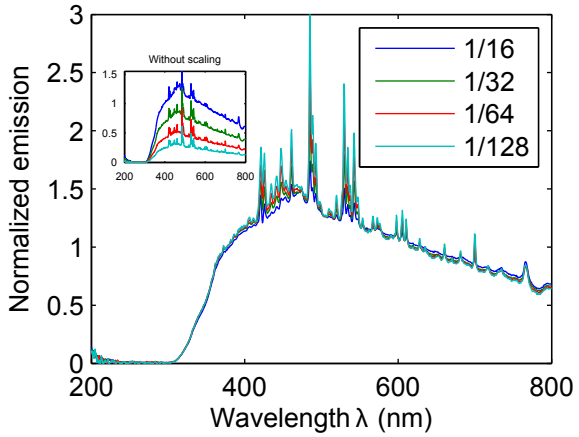

Figure 4. *Spectrum of the flash for varying intensities ($\frac{1}{16}$ to $\frac{1}{128}$); curves have been normalized.*

Our simultaneous measurement of the flash intensity with the camera and the spectral photometer enables us to relate both measurements as shown in Fig 5. We used a white plate as an object, a fixed optical bandpass filter at 550nm and acquired several images with the same flash intensity setting. The camera values are preprocessed by subtracting the black reference image and by application of the inverse CTF. We estimated a pulse-to-pulse variability of up to 42.5%, i.e., the gray level values range from 141.9 for the first flash in a sequence down to 81.6 for the last one. The flash intensity therefore decreases with consecutive triggers – although the flashgun prohibits triggers while recharging. The large intensity variations confirm the necessity of an external sensor for brightness calibration. We estimated the mean error between the spectral photometer and the camera measurements by computing the differences between the sensor values and a line of best fit shown in Fig. 5. Related to 256 gray levels (8 bit), the mean calibration error is 0.54 gray values, which corresponds to 0.21%. We therefore propose an external sensor as an adequate calibration device for our application.

[1] http://www.sigma-photo.com/

[2] Dr. Gröbel UV-Elektronik GmbH, Goethestrae 17, D-76275 Ettlingen, Germany

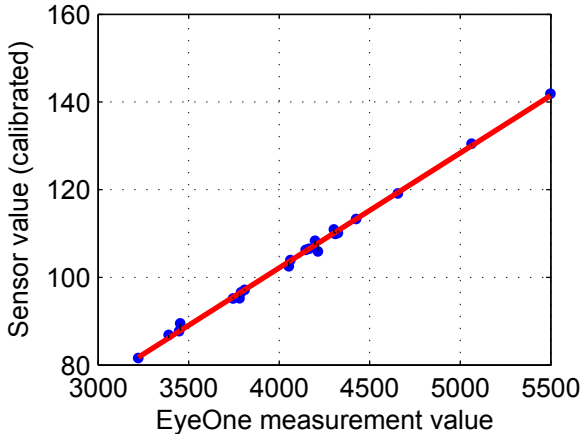

Figure 5. *Simultaneous measurement of the flash intensity with a spectral photometer and the camera.*

In addition to the intensity variations, we also detected a temporal illumination uniformity divergence. Towards this end we acquired several consecutive images of a white reference plate. For the preprocessing we subtracted the black reference image and applied the inverse CTF. To exclude the varying intensity of the images, we normalized them with the brightness in the center region. In Fig. 6, we additionally applied a common contrast stretch for two images to illustrate the uniformity divergence. The difference of the images in Fig. 6 (omitting the contrast stretch) is shown in the left image of Fig. 7. Relating to a center image intensity of 255 (8 bit), the differences range from -18 to +18, which is unacceptable for image acquisition. Our wide angle diffuser reduced the variations significantly and the differences of images for this case shown in Fig. 7 (right) range from -1.4 to 2.9.

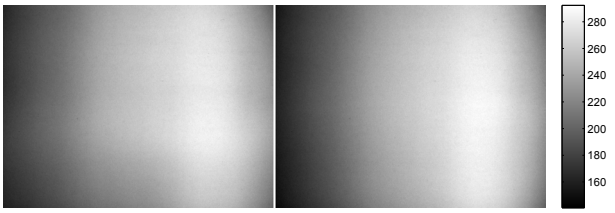

Figure 6. *Temporal variation of illumination uniformity for a setup without diffuser and without mirror; the contrast of both images has been stretched in the same manner.*

Especially when using the mirror shown in Fig. 2, we also discovered interference stripes in the images caused by constructive or destructive interference of waves. An example is depicted in Fig. 8, where the upper half represents the original image, whereas the lower half is contrast stretched to amplify the interference effect. The curve is a projection of the image in the vertical direction; we removed the global trend which is caused by the inhomogeneous illumination. The maximum range of the inference stripes is 3.62 gray values (related to 8 bit image values). Since the position of the stripes depends on the object position and therefore cannot be compensated for, they may slightly compromise the image. Without using a mirror the effect does

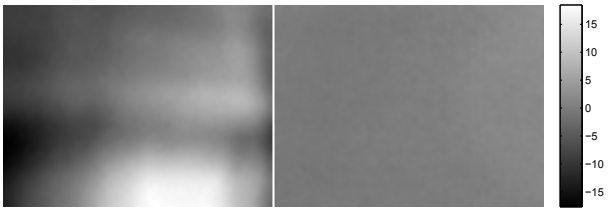

Figure 7. *Improvement of temporal illumination uniformity by usage of a wide angle diffusor: Difference between two consecutive images of Fig. 6 (left) and for the case using a wide angle diffuser (right).*

not appear in our setup. However, to improve illumination uniformity, we use the mirror.

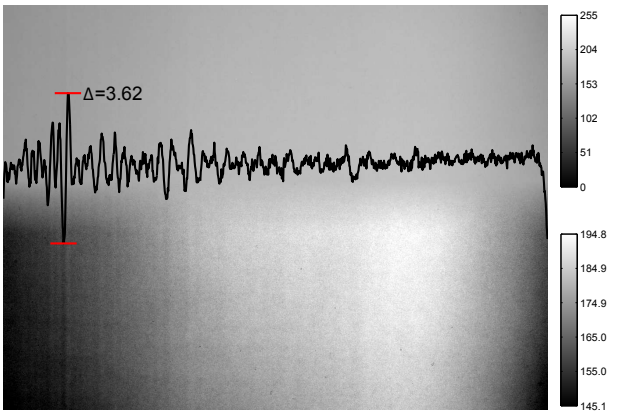

Figure 8. *Interference stripes caused by the flash light in combination with a mirror; original image and contrast enhanced version are split vertically.*

When using continuous light sources, the camera values relate to the exposure time of the camera since the light is integrated over the exposure time period. In contrast, flash light sources deliver their energy in a very short time; as long as the flash firing time is completely covered by the exposure, the exposure time itself has no effect. Therefore, the acquisition time can be shortened drastically when all components are synchronized. In our study we set the exposure time of the camera to one second. The measurement time of the EyeOne spectral photometer is approximately one second as well. We triggered both camera and photometer synchronously and fired the flash within one second. The linear relation between camera and photometer measurement in Fig. 5 confirms that synchronization works well – otherwise large stochastic errors would appear in the measurements.

Results

Our multispectral camera internally uses a Sony XCD-SX900 CCD grayscale camera with a chip size of 6.4mm × 4.8mm and a resolution of 1280 × 760 pixel. We use a Nikkor AF-S DX 18-70mm lens on the external F-mount, while the internal camera features a C-mount. The computer-controlled filter wheel between lens and imaging sensor features seven optical bandpass filters in the range between 400nm and 700nm, each with 40nm bandwidth. The consumer flashgun used in our experiment is a Sigma EF-500 DG Super. We measured the flash intensity with a GretagMacbeth EyeOne Pro spectral photometer. Other sensors could also be used. We used the flash intensity settings shown in Tab. 1 to achieve well-exposured images.

channel	1	2	3	4	5	6	7
intensity	$\frac{1}{4}$	$\frac{1}{8}$	$\frac{1}{16}$	$\frac{1}{16}$	$\frac{1}{16}$	$\frac{1}{8}$	$\frac{1}{4}$

Table 1: Flash intensity for each spectral channel.

We performed verification of our system by acquisition of a test chart (ColorChecker DC) with 237 color patches shown in Fig. 9 and the computation of the color error ΔE_{00} for each patch. The reference data was collected with our EyeOne Pro spectral photometer. Table 2 shows our examined configurations: As an alternative light source to the flashgun, we also used a halogen lamp with 100 watts at the same position and angle as the flashgun. We used *intrinsic* calibration as described in our section "Image Acquisition" using a reference patch within the acquired object and *extrinsic* calibration, relying on the external measurements of the flash intensity. Additionally, we also simulated both light sources by modeling the spectral path.

In the *extrinsic* calibration experiment, the resulting color error by using the flash light source is higher than the corresponding halogen acquisition. When comparing it to the second (*intrinsic*) experiment, where the calibration to the intensity of the light source is performed with a white patch in the image itself, the color errors produced by halogen and flash light are comparable. This means that the intensity variation of the flashgun introduces errors, even if the system is calibrated with an external sensor. With a perfect calibration, the results would yield the results from the second experiment. This is also confirmed by our simulation, which shows a similar accuracy for both light sources. Fig. 9 shows a detailed error report for each color patch when using the flash light source in experiment 2. As the histogram in Fig. 10 confirms, most of the colors are captured quite accurately with a color error $\Delta E_{00} \leq 2$. Due to a stray light or ghosting images [6], the black patches and some of the dark patches exhibit an increased color error. The glossy patches in column "S" of the ColorChecker DC also produce larger color errors.

	$\Delta\bar{E}_{00}$, flash	$\Delta\bar{E}_{00}$, halogen
extrinsic calibration	3.111	1.761
intrinsic calibration	1.594	1.761
simulation	0.844	0.937

Table 2: Color accuracy in terms of $\Delta\bar{E}_{00}$.

Conclusions

Our study shows promising results for image acquisition with a consumer flash light source with a mean color error of $\Delta\bar{E}_{00} = 1.594$ for a ColorChecker DC test chart. We have shown that the large intensity variations of the flashgun can be compensated by calibrating the images with the measurements of an external light sensor with a mean measurement error of only 0.21%. Calibration with a reference patch inside the acquired image works even better. We also investigated the large temporal variations of the illumination uniformity we reduced with a diffuser. Another critical point when using flash light sources – especially in combination with a mirror – are interference stripes arising from constructive or destructive interference of waves, which can not be compensated for.

It would be interesting to see the flash acquisition fully automated with flash exposure adaptation. Additionally, the external

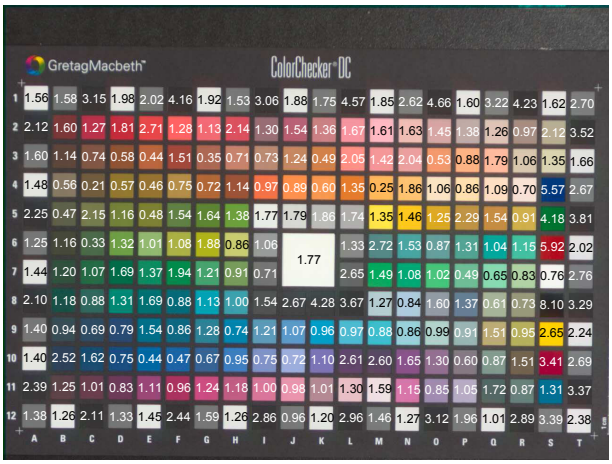

Figure 9. *Test chart acquired with a flash light source and the corresponding ΔE_{00} errors.*

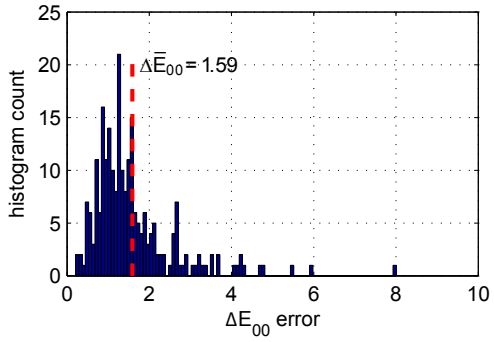

Figure 10. *Histogram of ΔE_{00} errors depicted in Fig. 9.*

measurement could be further improved to catch up with the intrinsic measurement.

Acknowledgments

The authors are grateful to B. Hill for many helpful discussions.

References

[1] A. Ribés, F. Schmitt, R. Pillay, and C. Lahanier, Calibration and spectral reconstruction for crisatel: An art painting multispectral acquisition system, Journal of Imaging Science and Technology, 49, pp. 563–573, Nov/Dec (2005).

[2] R. Berns, L. Taplin, M. Nezamabadi, M. Mohammadi, and Y. Zhao, Spectral imaging using a commercial color-filter array digital camera, Proc. The 14th Triennal ICOM-CC meeting, pp. 743–750, The Hague, The Netherlands, Sep (2005).

[3] J. Brauers, N. Schulte, and T. Aach, Modeling and compensation of geometric distortions of multispectral cameras with optical bandpass filter wheels, Proc. 15th European Signal Processing Conference, pp. 1902–1906, Poznań, Poland, Sep (2007).

[4] J. Brauers, N. Schulte, A. A. Bell, and T. Aach, Multispectral high dynamic range imaging, Proc. IS&T/SPIE Electronic Imaging, San Jose, California, USA, Jan (2008).

[5] S. Helling, E. Seidel, and W. Biehlig, Algorithms for spectral color stimulus reconstruction with a seven-channel multispectral camera, Proc. IS&Ts 2nd European Conference on Color in Graphics, Imaging and Vision CGIV 2004, pp. 254–258, Aachen, Germany, Apr (2004).

[6] J. Brauers and T. Aach, Modeling and compensation of ghosting in multispectral filter wheel cameras, IEEE Southwest Symposium on Image Analysis and Interpretation, Santa Fe, New Mexico, USA, Mar (2008). Accepted for publication.

Author Biography

Johannes Brauers received his diploma degree in Electrical Engineering from RWTH Aachen University, Germany, in 2005. Since then he is with the Institute of Imaging and Computer Vision, RWTH Aachen University as a Ph.D. student. His current research interests are multispectral imaging, in particular modeling and compensation of geometric distortions, high dynamic range imaging and identification of the camera transfer function. He received the "EADS Defence Eletronics ARGUS Award 2005" for his master thesis.

Stephan Helling received his diploma degree in Electrical Engineering from RWTH Aachen University in 2001. He is now engaged in research on multispectral imaging systems with focus on multispectral cameras at the same university as a member of the Color and Image Processing Research Group. He is member of IS&T and the German Society for Color Science and Application DfwG.

Til Aach is Head of the Institute of Imaging and Computer Vision, RWTH Aachen University. From 1993 to 1998, he was with Philips Research Laboratories. From 1998 to 2004, he was a Full Professor and Director of the Institute for Signal Processing, University of Luebeck, Germany. His research interests are in medical and industrial image processing, signal processing, pattern recognition, and computer vision. He has authored or co-authored over 200 papers, and is a co-inventor for about 20 patents.